JOURNAL OF MATERIALS SCIENCE 28 (1993) 4974–4982

Thermal expansion behaviour of thermoplastic composites

Part II

J. A. BARNES
ICI Fibres, Wheatley Hall Road, Doncaster DN2 4LT, UK

The thermal-expansion behaviours of a variety of thermoplastic composites based on the ICI Victrex polymers PEEK, ITA, HTA and ITX are examined. It is shown that when each of the composites is raised above the glass-transition temperature, T_g, of the polymer matrix considerable permanent distortion occurs in the small samples used, though the effect is not evident below T_g. This is attributed to relaxation of process-induced residual stresses generated in the larger plates from which the samples were prepared. A number of models are used to calculate the thermal-expansion behaviour of the fibres transverse to their long axes; the results are shown to be inconsistent, and in poor agreement with directly measured properties. Finally, the utility of the data for calculation of thermal-expansion behaviour parallel to the fibres in the composites is considered.

1. Introduction

The thermal-expansion behaviour of thermoplastic composites of the ICI Aromatic Polymer Composite (APC) family is a subject which has received periodic attention over the past few years [1–5]. However, a review of earlier work reveals that the primary interest has been the behaviour of such materials in the direction parallel to the fibres (i.e. in a direction in which measurement is difficult), whilst the "easier" measurements transverse to the fibres have been largely ignored. In addition, with the exception of some measurements on the composite HTA [4], only data for PEEK composites have been reported.

The aim of this report is to summarize the most recent collection of thermal-expansion data relating to the complete range of thermoplastic matrices available from ICI Fiberite, and to place these data in context with earlier work.

2. Theory

The prediction of thermal-expansion behaviour of composite materials is an exercise which has undergone constant refinement over the past quarter of a century (see [6] for an excellent review). Parallel to the fibre direction in carbon-fibre-reinforced materials, the overall behaviour of the composite is heavily dominated by the fibres themselves, which have high stiffness and a negative coefficient of thermal expansion (CTE) along their length [1–6]. Due to the overriding effect of the fibres it is often sufficiently accurate to use a simple rule-of-mixtures equation for predictive purposes [7]:

$$\alpha_{11}^{c} = \frac{\alpha_{11}^{f} E_{11}^{f} V_f + \alpha_m E_m V_m}{V_f E_{11}^{f} + V_m E_m} \quad (1)$$

where the subscript m denotes matrix, the superscript f denotes fibre, 11 denotes the direction parallel to the fibres, and the remaining terms have their usual meanings. Equation 1 was obtained for isotropic constituents having equal Poisson's ratios. Schapery [8] showed that the relationship also gives a good approximation of thermal expansion when the Poisson's ratios of the constituents differ.

The behaviour transverse to the fibre direction is more difficult to predict from the basic constituent performance; this is usually attributed to changes in phase geometry and distribution in the radial direction. Chamberlain [9] developed a relationship considering each fibre as being surrounded by a matrix in the form of a thick-walled cylinder:

$$\alpha_2^{c} = \alpha_m + \frac{2(\alpha_2^{f} - \alpha_m)V_f}{\nu_m(F - V_f) + (F + V_f) + (1 - \nu_{12}^{f})(F - V_f)E_m/E_f} \quad (2)$$

where F represents the packing fraction of the fibres, equal to 0.9609 for hexagonal close packing, and to 0.7854 for square packing. In a rather neater analysis, Schapery [8] obtained, for an upper-bound value, the relationship:

$$\alpha_2^{c} = (1 + \nu_m)\alpha_m V_m + (1 + \nu_f)\alpha_f V_f - \alpha_{11}^{c}(\nu_f V_f + \nu_m V_m) \quad (3)$$

in which the behaviour of the composite parallel to the fibres is also included. The Schapery relationship is applicable to the case of isotropic components in an orthotropic composite, though other workers have reasonably argued that the expression is not complete

and requires the addition of a second fibre term to allow extension to fibre anisotropy thus [6]:

$$\alpha_2^c = (1 + \nu_m)\alpha_m V_m + \alpha_{2f} V_f + \alpha_{1f} \nu_{12}^f V_f - \alpha_{11}^c(\nu_f V_f + \nu_m V_m) \quad (4)$$

which was shown to give accurate results for Kevlar/epoxy composites. The relationships above give reasonable approximations for the behaviour of unidirectional materials in the principal orientation directions. However, the work presented on thermoplastic composites by Barnes *et al.* [1–3] indicates that the analyses of Schapery and Chamberlain fail to give good agreement when measured values of the thermal expansion behaviour of composites are used to calculate the thermal expansion coefficient of the fibres in such materials; the difference can be as high as a factor of two. Back-calculation by this means is a dangerous undertaking since the modified analysis of Schapery and the work of Chamberlain only provide bounds on transverse thermal expansion behaviour; observation suggests that other analyses may be more appropriate.

Later work on the prediction of thermal expansion behaviour extended the energy approach used by Schapery. Rosen developed a process for the calculation of the behaviour of a system made from isotropic constituents [10] to an anisotropic model [11, 12] with the following result:

$$\alpha_{ij}^* = \bar{\alpha}_{ij} + P_{klrs}(S_{rsij}^* - \bar{S}_{rsij})(\alpha_{kl}^{(1)} - \alpha_{kl}^{(2)}) \quad (5a)$$

$$P_{klrs}(S_{rsij}^{(1)} - S_{rsij}^{(2)}) = I_{hkij} \quad (5b)$$

where α_{ij}^* = effective thermal expansion coefficients, S_{rsij}^* = effective elastic compliances, $\alpha_{ij}^{(1,2)}$ = phase thermal expansion coefficients, $S_{rsij}^{(1,2)}$ = phase elastic compliances, and I_{ijhk} = fourth-rank symmetric unit tensor.

Assuming macroscopic and microscopic transverse isotropy, the effective property tensors required for substitution into Equation 5 are:

$$S_{1111}^* = \frac{1}{E_{11}}, \quad S_{2222}^* = \frac{1}{E_{22}}$$
$$S_{1122}^* = -\frac{\nu_{12}}{E_{11}}, \quad S_{2233}^* = -\frac{\nu_{21}}{E_{22}} \quad (6)$$
$$S_{1212}^* = \frac{1}{4G_{12}}, \quad S_{2323}^* = \frac{1}{4G_{23}}$$

and all other components vanish. In addition, an approach based on the method of cells has been provided by Aboudi [12], and a three-phase model has been developed by Christiensen [13], though these will not be reviewed here.

If data for the behaviour transverse and parallel to the fibres are available then the CTE at any angle, θ, to the fibre direction in a unidirectional composite has been shown by Pirgon *et al.* [14] to be given by:

$$\alpha_\theta = \alpha_1^c \cos^2\theta + \alpha_2^c \sin^2\theta \quad (7)$$

Which has been proven to be valid for PEEK composites by Barnes *et al.* [1–3].

TABLE I Materials

Material	Polymer, T_g (°C)	Fibre type	Fibre tensile modulus (GPa)
AS4/PEEK	143	Hercules AS4	234
IM7/PEEK	143	Hercules IM7	303
IM8/ITX	175	Hercules IM8	317
IM8/HTA	260	Hercules IM8	317
IM8/ITA	210	Hercules IM8	317

3. Experimental procedure

3.1. Materials

Laminates were prepared from four composite pre-impregnated materials reinforced with Hercules intermediate-modulus fibres, and one reinforced with Hercules AS4 fibres. The following matrices were used: Polyarylether etherketone (PEEK), "Victrex" Intermediate Temperature Semicrystalline Polymer, ITX (an aromatic copolymer), Victrex Intermediate Temperature Amorphous Polymer ITA (a polyether sulphone) and Victrex High Temperature Amorphous Polymer HTA (a bisphenyl-modified polyether sulphone). A summary of the materials is shown in Table I. In each case the composite was prepared by ICI Fiberite using a proprietary impregnation process, and 300 × 300 mm 32-ply uniaxial laminates were prepared in an autoclave using the manufacturer's recommended processing cycle. An autoclave was required to ensure that the semi-crystalline materials achieved their full crystallinity, thus preventing discontinuities in behaviour during measurement. A series of samples approximately 13 mm long and 5 mm wide were cut from the centre of each plate using a diamond saw, with the principal fibre axis at 90°, 60° or 30° to the long axis of the sample. The samples were dried, then stored in sealed polyethylene bags prior to testing.

3.2. Procedure

Measurements of the thermal-expansion behaviour were then carried out in a conventional Perkin-Elmer TMA push-rod-type dilatometer, with a heating rate of 5 °C min^{-1} and a normal load of 15 mN. The data were then reduced to thermal-expansion coefficients for the materials using a personal-computer-based spreadsheet program. In all cases instantaneous values of the CTEs were calculated over 2 °C temperature increments, using the immediately preceeding length of the sample as the initial length.

4. Results

Since most work to date has focused on the behaviour of Hercules-AS4-fibre-reinforced PEEK, the behaviour of this material will be examined in the most detail, and it will be used as a vehicle to describe the response of other materials. In most respects the behaviour of all materials was similar.

4.1. Behaviour of AS4/PEEK

Fig. 1 shows the change in length of an AS4/PEEK composite rod as a function of temperature over a

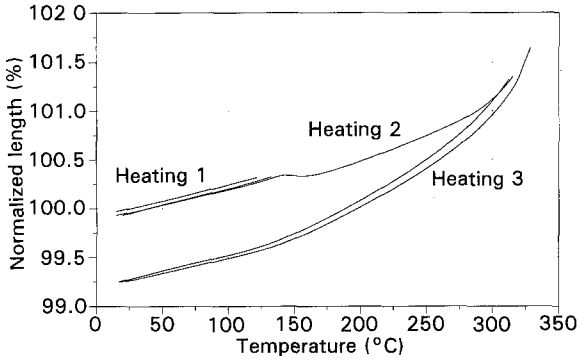

Figure 1 Change in the normalized length with temperature and thermal cycling for PEEK/AS4 at 90° to the fibre direction.

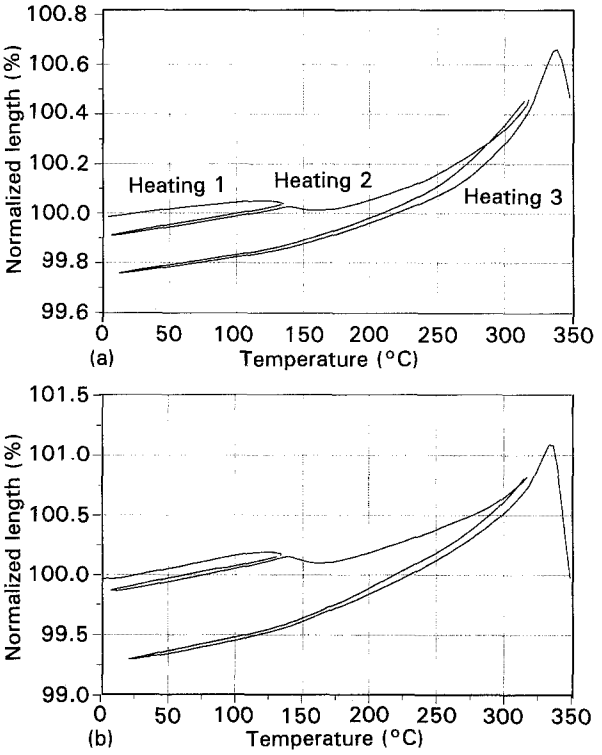

Figure 2 Change in normalized length with temperature and thermal cycling for PEEK/AS4 at: (a) 60° and (b) 30° to the fibre direction.

number of heating cycles. Data are presented in terms of normalized length, that is, the instantaneous length divided by the original length, and for convenience the length is given as a percentage. The behaviour is rather unusual, and follows a pattern not previously reported. The initial heating cycle, to a point approximately 10 °C below the glass transition, T_g, of the polymer (143 °C) and back to room temperature, is approximately linear (with a slightly reduced gradient near to the T_g. Cooling follows essentially the same path as heating, and the overall cycle shows little hysteresis. Behaviour of this type has been reported in [1–3]. On the second cycle (heating 2), which is to 310 °C (almost into the melt region for PEEK), a significant reduction in length is observed as the composite passes through the T_g, and on cooling a very considerable permanent length reduction is observed. Subsequent heating to the melt produces a trace which closely follows the cooling path; a final cooling trace is not recorded due to sample melting. Behaviour of this type was noted for all AS4/PEEK composites, though the magnitude of the effect was reduced in the less matrix dominated 60° and 30° samples – a summary is shown in Fig. 2. The origin of this effect will be discussed more fully below.

Reducing the data shown in Fig. 1 to the form of CTEs reveals the effect more strongly, since in effect the CTE/temperature curve is a plot of the gradient of Fig. 1 against temperature. Fig. 3a to c shows each of the subsequent heat/cool traces expressed in terms of the CTE and Fig. 3d shows all of the results superimposed. What is perhaps most surprising is the fact that, despite the rather massive discontinuities in the curves around T_g on the first and second cycles, if the sample length at the start of each cycle is used as the starting point for the CTE calculations then overall the absolute value of the CTE varies little. Since part of the aim of this work was to provide CTE data for other experimental purposes, values from each of the sample examined were taken from the final heating trace, and these are summarized as mean values in Table II, and as a final plot in Fig. 4. The curve shows increases near the PEEK T_g and near the onset of melting at 310 °C, as expected. However, note that the behaviour above approximately 325 °C, where a rapid fall in CTE is recorded, is not reasonable since the thermal-expansion coefficient of the matrix (which dominates the overall behaviour) is still increasing. This fall simply reflects the loss of integrity of the sample, and data above this point should not be considered useful. As a consequence of this, in Table II all data which were recorded as either zero or negative values are ignored. The thermal-expansion behaviour at angles 90°, 60° and 30° to the fibre direction is summarized in Fig. 5.

Fig. 6 shows the change in length as a function of thermal cycling for the IM7/PEEK composite; the behaviour is essentially identical to that of the AS4-reinforced material, and in the interests of space data for the 60° and 30° samples will not be presented. Fig. 7 shows the mean, final-cycle, thermal-expansion trace superimposed on the trace for AS4/PEEK. As expected, there is considerable similarity between the responses, though the absolute value of the CTE for the IM7-reinforced material is marginally lower at all temperatures. The final semi-crystalline polymer composite examined was Victrex ITX reinforced with Hercules IM8 fibres. Fig. 8 shows a typical length/thermal cycle plot for a sample with the fibres at 90° to the sample axis. Again, the behaviour is similar to that for IM7/PEEK, with the exception that the onset of sample shrinkage is delayed until a higher temperature. The mechanical properties of IM7 fibres are similar to those of IM8 (Table I), and the only significant difference between PEEK and ITX in terms of their thermomechanical behaviour is an increase in the glass-transition temperature in the case of ITX. Hence it may reasonably be expected that the overall thermal expansion behaviour near room temperature will be similar to that of the PEEK composite, but with a lower absolute value. This expectation is ful-

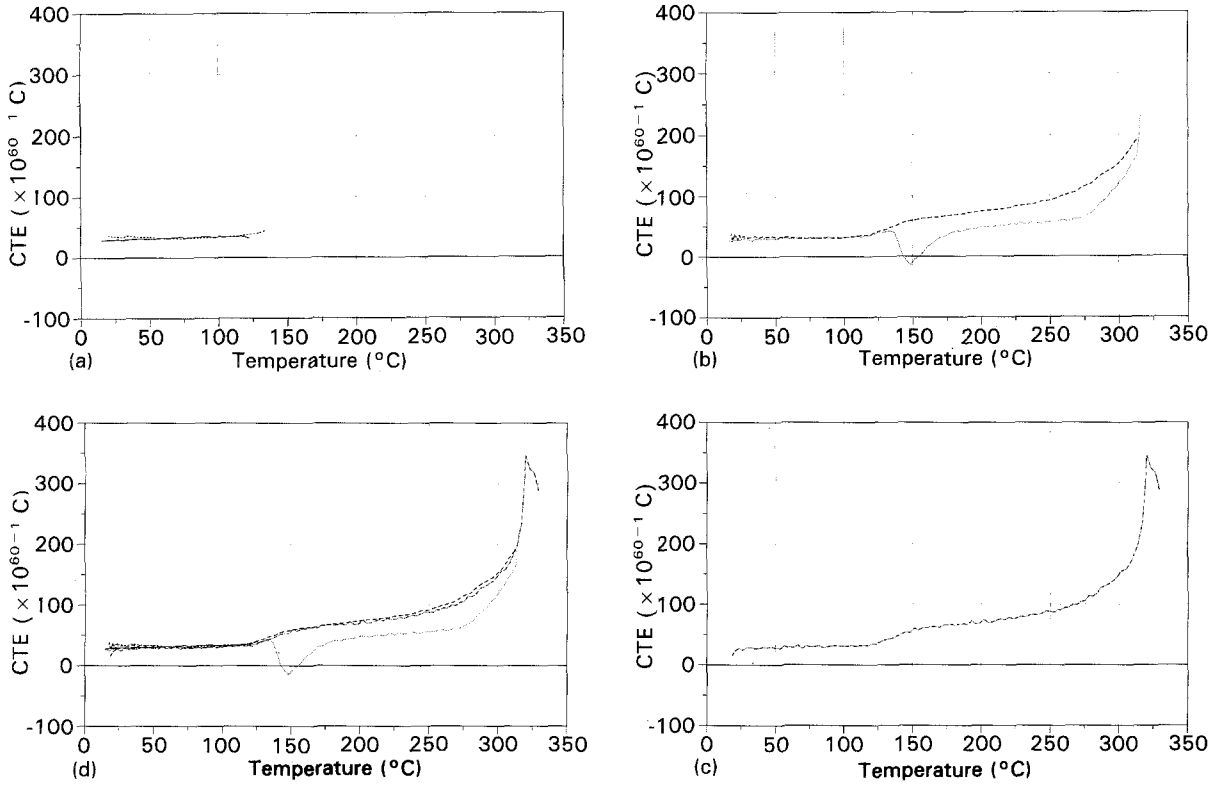

Figure 3 Linear CTE for PEEK/AS4 at 90° to the fibre direction. (a) The first thermal cycle (——) heating cycle 1, and (– – –) cooling cycle 1. (b) The second thermal cycle: (. . .) heating cycle 2, and (– – –) cooling cycle 2. (c) The third thermal cycle: (– · · –) heating cycle 3. (d) A summary plot over all thermal cycles.

TABLE II Mean values of the CTE for all materials from 20 °C to T_g

Temperature (°C)	Linear CTE ($\times 10^{-6}$ °C^{-1})				
	APC2/AS4	APC2/IM7	ITX/IM8	HTA/IM8	ITA/IM8
20	29.57	27.40	25.71	29.00	28.97
30	30.48	28.77	26.09	29.89	29.63
40	30.79	27.74	27.31	31.11	30.09
50	31.10	29.77	26.68	31.34	30.56
60	31.30	30.26	27.29	30.86	30.52
70	31.49	29.82	28.58	32.21	31.04
80	31.62	31.15	27.90	32.94	31.48
90	31.74	31.40	28.47	33.11	31.89
100	32.60	30.71	28.79	33.91	32.26
110	33.46	31.22	29.13	33.56	32.07
120	36.13	34.40	28.30	33.54	32.72
130	38.80	40.21	29.97	34.00	33.00
140	48.46	49.87	31.30	34.09	33.23
150	58.12	58.93	32.63	34.88	33.69
160	59.22	62.40	38.21	35.13	34.12
170	60.32	65.38	47.56	35.40	34.56
180	62.36	68.91	56.61	35.85	34.82
190	64.39	66.47	60.28	36.08	38.38
200	67.53	70.96	63.59	37.26	46.52
210	70.67	73.00	65.97	37.13	75.20
220	73.72	76.78	69.14	38.30	5.87
230	76.77	79.81	71.03	44.81	–
240	80.98	82.67	75.36	65.55	–
250	85.19	84.89	80.26	57.27	–
260	87.13	95.04	83.43	–	–
270	89.08	98.85	91.32	–	–
280	93.34	108.85	98.85	–	–
290	97.61	118.38	108.53	–	–
300	130.77	140.07	119.40	–	–
310	163.93	164.13	136.02	–	–
320	231.66	323.03	180.13	–	–
330	299.38	302.87	184.00	–	–
340	–	–	202.00	–	–

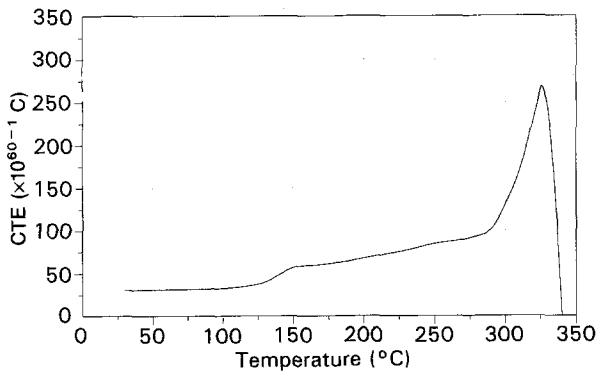

Figure 4 Linear CTE for PEEK/AS4 at 90° to the fibre direction as the mean of all final thermal cycles.

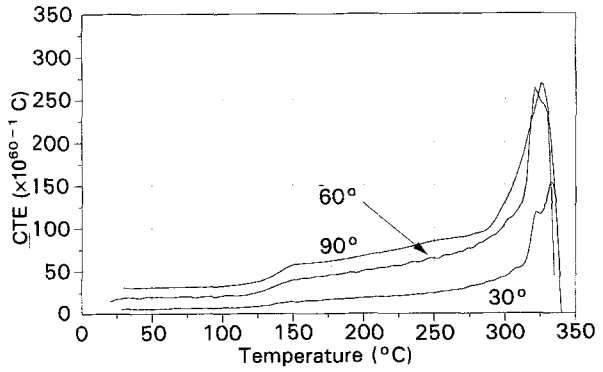

Figure 5 Linear CTE for PEEK/AS4 at 30°, 60° and 90° to the fibre direction as the mean of all final thermal cycles.

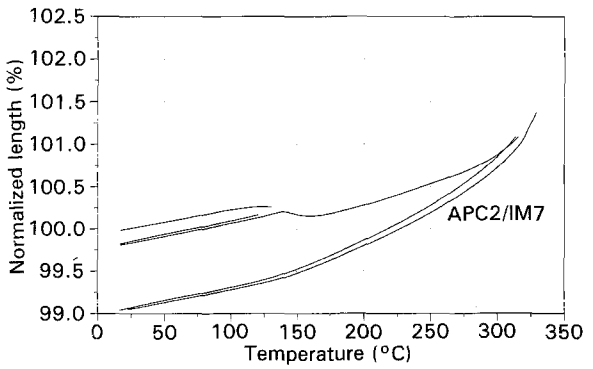

Figure 6 Change in the normalized length with temperature and thermal cycling for PEEK/IM7 at 90° to the fibre direction.

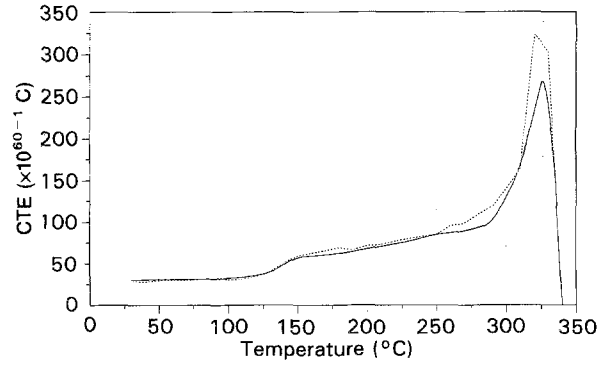

Figure 7 Comparison of the thermal-expansion behaviour of (——) PEEK/AS4 and (– – –) PEEK/IM7 at 90° to the fibre direction.

filled in Fig. 9, which shows a comparison of the final-cycle mean-value plot of the linear CTE of ITX/IM8 and PEEK/IM7. The increase in CTE at the T_g is delayed in the case of ITX, as is the rapid rise in the CTE near the onset of melting. Fig. 10 shows the mean response at 90°, 60° and 30° to the fibre direction.

Finally, Figs 11 and 12 show typical length/temperature traces for IM8-fibre-reinforced HTA and ITA composites, respectively. In each case the examples shown contain fibres at 90° to the long axis of the sample, and the thermal cycles follow a similar pattern – initial heating to just below T_g, a second cycle to the quoted T_g for each material, and then a final cycle through T_g. Since each of the final sample types

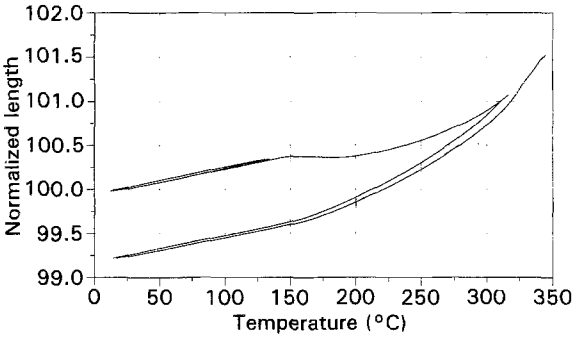

Figure 8 Change in the normalized length with temperature and thermal cycling for ITX/IM8 at 90° to the fibre direction.

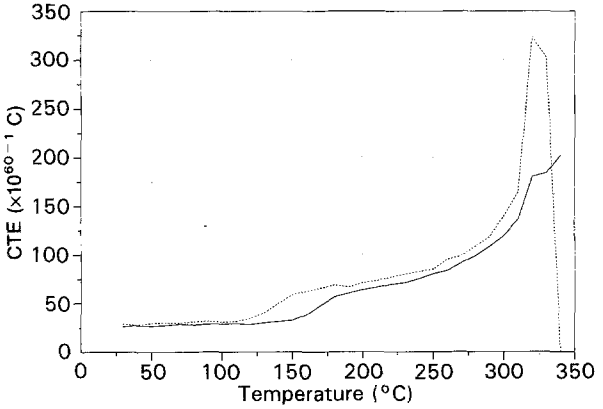

Figure 9 Comparison of the thermal-expansion behaviour of (– – –) PEEK/IM7 and (——) ITX/IM8 at 90° to the fibre direction.

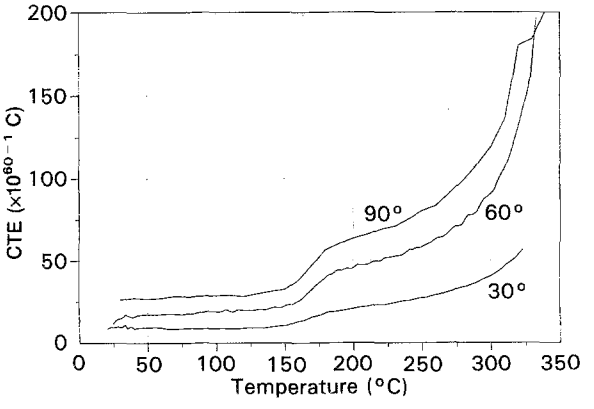

Figure 10 Linear CTE of ITX/IM8 at 30°, 60° and 90° to the fibre direction as a mean of all final thermal cycles.

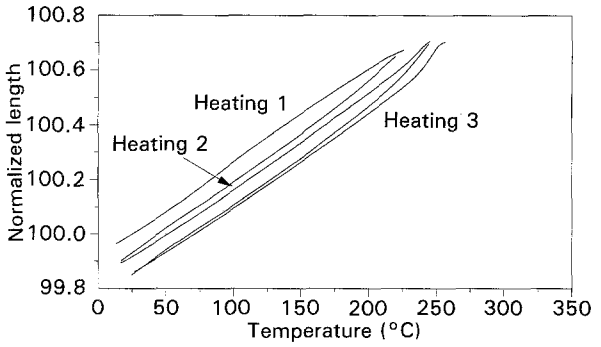

Figure 11 Change in the normalized length with temperature and thermal cycling for HTA/IM8 at 90° to the fibre direction.

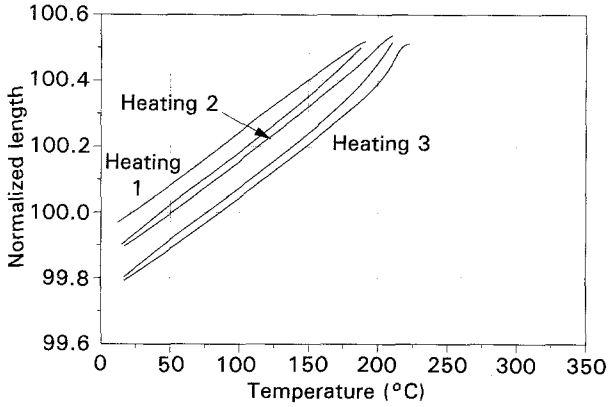

Figure 12 Change in the normalized length with temperature and thermal cycling for ITA/IM8 at 90° to the fibre direction.

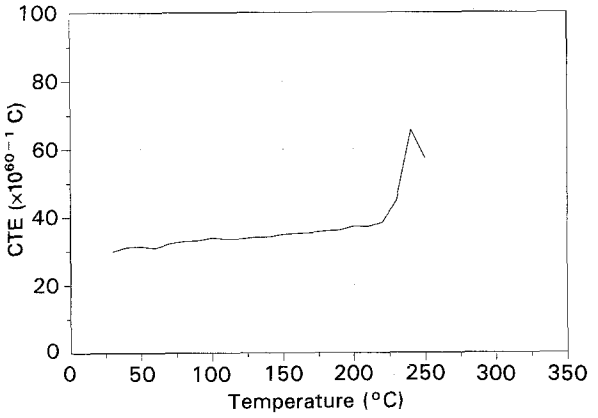

Figure 13 Linear CTE for HTA/IM8 at 90° to the fibre direction as a mean of all the final thermal cycles.

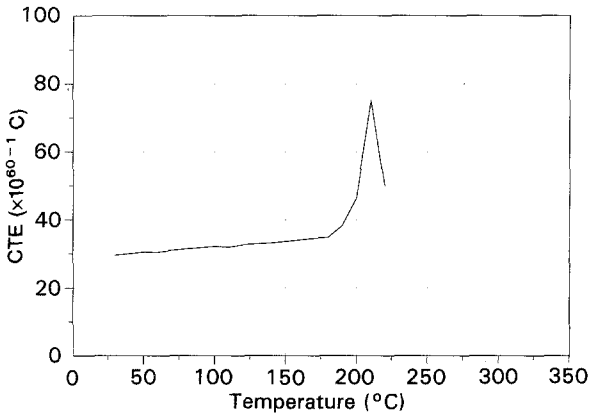

Figure 14 Linear CTE for ITA/IM8 at 90° to the fibre direction as a mean of all the final thermal cycles.

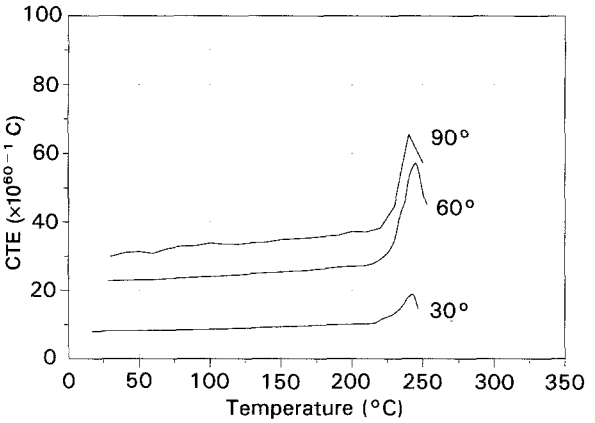

Figure 15 Linear CTE for HTA/IM8 at 30°, 60° and 90° to the fibre direction as a mean of all the final thermal cycles.

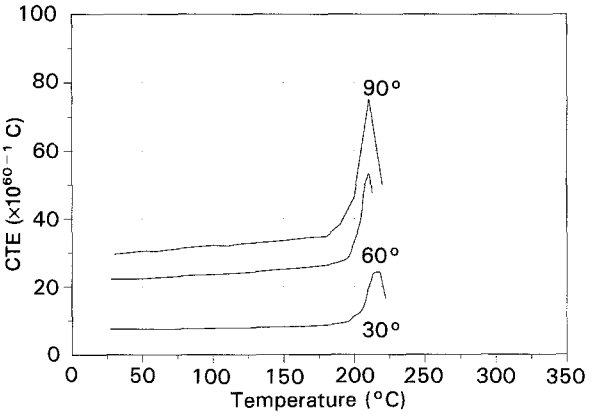

Figure 16 Linear CTE for ITA/IM8 at 30°, 60° and 90° to the fibre direction as a mean of all the final thermal cycles.

contain amorphous polymers, rather than semi-crystalline materials as in the three former cases, passing through the T_g results in melting, hence the major difference between these plots and those for PEEK and ITX.

Length/temperature data are reduced to final-cycle mean CTE results in Figs 13 and 14, and a summary of mean responses at 90°, 60° and 30° to the fibre directions is shown in Figs 15 and 16 for each of the amorphous materials.

5. Discussion

Three areas relating to the data presented must be treated in this analysis. Firstly, the significant, permanent length change recorded in each of the samples requires explanation; secondly, the utility of the models outlined above for prediction of behaviour should be considered; and finally, the utility of these data must be considered.

The permanent set in each of the samples is an interesting phenomenon, and although this has not been reported in the thermoplastic composites in the past, work by Farrow *et al.* on PEEK polymer [16] has revealed similar, but not identical behaviour. There are several possible reasons why a reduction in sample length may occur, and these are discussed individually below.

In the case of semi-crystalline polymers a thermal excursion into the region where further crystallization is possible will result in an increase in density, and a reduction in volume. In the case of the samples tested here only PEEK and ITX are capable of crystallizing, and care was taken to ensure that full crystallization took place on the rather slow cooling from the melt caused by the use of an autoclave. A comparison of the degree of crystallinity of the PEEK sample measured by differential scanning calorimetry before and after testing revealed insignificant differences, and whilst this may have had a small effect on the behaviour of semi-crystalline materials, the response of the amorphous polymers HTA and ITA must be independent of this effect. A second consideration is moisture absorption. One would naturally expect this to be most significant in the case of amorphous polymers, and experimental work on ITA composites both as-received and after drying for 24 h at 60 °C in vacuum revealed no significant change in behaviour. The final likely explanation for such behaviour in all samples is the influence on residual stresses induced during processing. Whilst this subject has been considered in the case of biaxial and rapidly formed laminates [17–20], it must be remembered that the act of applying normal compression to a laminate in the melt induces strains in the plane of the laminate, which can be relaxed at high temperatures.

Figs 17 to 19 illustrate the change in length during the initial heating cycle of samples of AS4/PEEK composite cut from the same laminate used to provide all other samples. The final temperature was 250 °C in each test. In this case examination of the sample behaviour was carried out parallel to the fibres (Fig. 17), at 90° to the fibre in the plane of the laminate (Fig. 18) and at 90° to the fibre out of the plane of the laminate (Fig. 19). It is quite apparent that whilst the sample is contracting significantly within the plane, there is a significant out-of-plane increase in size. Fig. 20 shows the change in volume (expressed as the normalized volume) with temperature calculated from these data. The lack of any disturbance in the smooth curve as the material passes through the glass transition suggests that the behaviour is due simply to a relaxation process, and it would appear that the cause of this behaviour is process-induced residual stresses. In earlier work [1–3] all samples were cut from much smaller plaques of composite (approximately 50 by 150 mm), and consequently the likelihood is that the size of the laminate used to provide material for testing has affected the behaviour, which appears reasonable. However, there is scope for further study of this phenomenon.

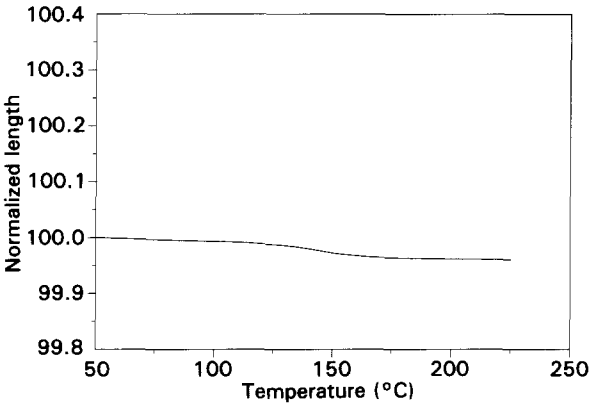

Figure 17 Change in normalized length for PEEK/AS4 parallel to the fibre direction.

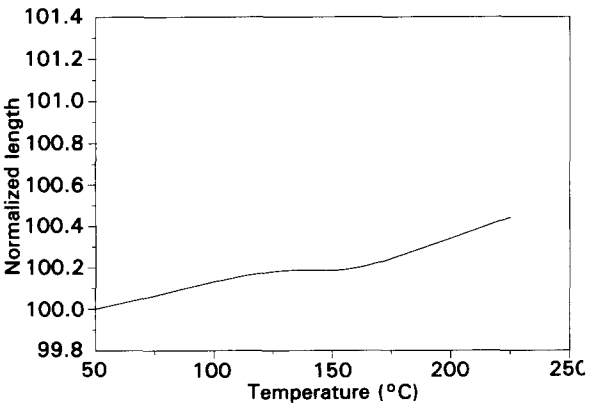

Figure 18 Change in normalized length for PEEK/AS4 at 90° to the fibre direction in the plane.

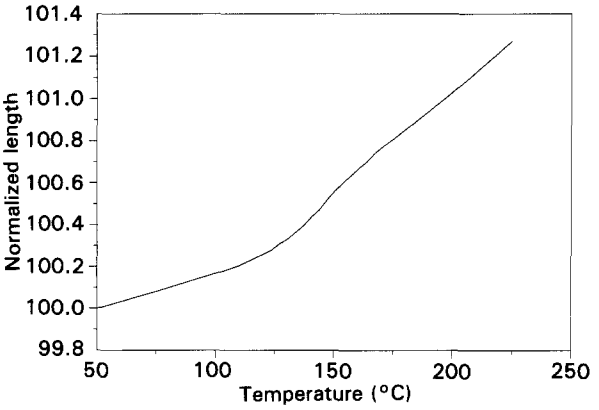

Figure 19 Change in normalized length for PEEK/AS4 at 90° to the fibre direction out of the plane.

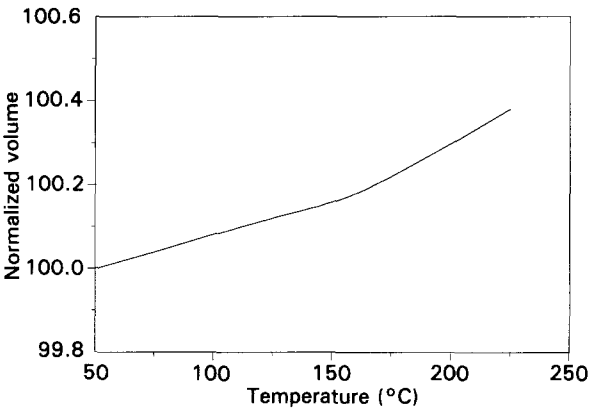

Figure 20 PEEK/AS4, normalized volume based on data from Figs 17–19.

5.1. Comparison with theory

In order to simplify discussion of this area, it is appropriate that calculations of material behaviour at room temperature only are presented, since it is in this

TABLE III Calculated fibre transverse CTE at 23 °C

Fibre	Calculated linear CTE ($\times 10^{-6}$ °C^{-1}) at 23 °C			
	Chamberlain [9]		Modified Schapery [8]	Rosen and Hashin [11]
	Square packing model	Hexagonal packing model		
Hercules AS4	26.1	22.4	36.3	22.7
Hercules IM7	23.5	19.4	36.2	20.1
Hercules IM8	23.0	18.27	38.4	21.5

region that the behaviour of the constituents have been most accurately characterized. In order to calculate the thermal-expansion behaviour of a composite material it is necessary to have an accurate measure of the behaviour of each of the individual constituents. In the case of materials reinforced with carbon fibres, the difficulties lie in the absolute determination of properties transverse to the long axis, since such fibres are typically only 5–7 μm in diameter. Particular difficulties lie in the measurement of the thermal-expansion behaviour of fibres in this direction, and in consequence rather than using uncertain data to calculate measured properties it is more interesting to use the composite data to back-calculate the fibre CTE. Table III shows the calculated transverse CTE of each of the fibres tested based on measurements from the PEEK and HTA composites using the transverse fibre properties in Table IV (which are drawn from a variety of sources) and resin data from [1–4]. As described in previous work [1–3] there is a significant discrepancy between the "classical" studies of Chamberlain and Schapery, and it is interesting to note that the rather more satisfactory analysis of composite behaviour due to Rosen provides results close to those of Chamberlain. Whilst it is not possible to deduce which result is correct (indeed, all data are much greater than the typical values of around 12×10^{-6} °C^{-1} measured by Sheaffer in one of the few single-fibre experiments reported [21]) this comparison is useful in that it implies that the Chamberlain and Rosen analyses are more appropriate for a first-level estimation of the behaviour of materials of this type. However, note that the fibre properties used for the calculations, and presented in Table 4, are only estimates based on composite performance. Nonetheless the reason why there is such a discrepancy between the three analyses and the single directly measured value of fibre CTE is unclear, and is worthy of further study.

TABLE IV Fibre properties

Property	Hercules AS4	Hercules IM7	Hercules IM8
E_{11} (GPa)	234	303	317
E_{22} (GPa)	15	15	15
G_{12} (GPa)	20	20	20
G_{23} (GPa)	5	5	5
ν_{12}	0.25	0.25	0.25
ν_{21}	0.013	0.013	0.013
α_1 ($\times 10^{-6}$ °C^{-1})	0.24	− 0.16	− 0.16
α_2 ($\times 10^{-6}$ °C^{-1})	See text	See text	See text

5.2. Utility of data

Whilst the data presented here have use in the prediction and understanding of the behaviour of each of the materials examined, it is noticeable that no measurements have been performed parallel to the fibre direction in the materials. This is due to the fact that the accuracy of push-rod dilatometers is of the same order as the thermal-expansion coefficient of the materials themselves, and in consequence the errors in the data make their use unsatisfactory. Further, earlier work [1–3] has shown that the CTE of PEEK composites of the type examined here is essentially zero up to the T_g, and work in [20] appears to verify that the assumption of zero CTE parallel to the fibres up to the melt is reasonable. However, Equation 7 provides a relationship between the thermal-expansion coefficient of a

TABLE V Calculated values of the CTE parallel to the fibre direction

Material	Calculated α_{11} ($\times 10^{-6}$ °C^{-1})		Measured α_{11} ($\times 10^{-6}$ °C^{-1})
	Based on 30° data	Based on 60° data	
PEEK/AS4	+ 0.147	− 4.515	0.229 [2], 0.270 [4]
PEEK/IM7	− 0.313	− 4.734	− 0.181 [2]
ITX/IM8	− 0.900	− 5.646	–
HTA/IM8	− 0.750	− 2.130	− 0.05[a] [4]
ITA/IM8	− 0.076	− 2.432	–

[a] Datum for IM6/HTA

laminate at some angle, θ, to the behaviour in the principal axes, and this relationship has been verified for carbon-fibre-reinforced PEEK [1–3]. Hence there is interest in attempting to use these data to provide an estimate of behaviour parallel to the fibres.

Table V shows the calculated values of CTE based on the properties of the composite at 90° in combination with each of the other angular data. Measured data are also shown where available. One would expect the data generated at 60° to the fibre direction to provide the best estimate of CTE parallel to the fibres when used in combination with the 90° data, since the length change in such samples should be greater than those in the 30° samples, and thus more accurately recorded. However, the 30° data appear to provide a better estimate of the 0° response, for reasons which are not entirely clear. Whilst the estimates provided by the 30° results are reasonable, it must be concluded that this approach is not recommended.

6. Conclusion

Data for the thermal-expansion behaviour at 90°, 60° and 30° to the fibre direction in five thermoplastic composites are presented. It is shown that in the case of small samples cut from the centre of large plates there is considerable permanent shrinkage in the plane of the sample when raised above the polymer T_g in each of the materials examined. A variety of possible causes are considered, and the effect is attributed to the relaxation of process-induced residual stresses. Three models for the thermal-expansion behaviour of composites are used to calculate the transverse CTE of the reinforcing fibres, based on the recorded data. It is shown that two of the models provide similar values for this property, though each of the models results in a value much greater than that expected from the data measured. Finally, the possibility of using data generated at angles to the fibre axis to calculate the CTE parallel to the fibres in a composite is considered, and rejected.

Acknowledgements

The author would like to thank the following for their contributions to this work: A. Broadhurst, P. Willcocks, I. Luscomb, N. Zahlan, I. Simms and N. Cogswell of ICI Wilton; D. Leach, T. McDaniels, G. Byerly, B. Moreira, and R. Yost of ICI Tempe; Professor B. Yates and Dr G. Wostenholm of Salford University.

References

1. J. A. BARNES, I. J. SIMMS, G. J. FARROW, D. JACKSON, G. WOSTENHOLM and B. YATES, Proceedings of the American Society for Composites Fourth Technical Conference Technomic, (1989) 717–725.
2. J. A. BARNES, I. J. SIMMS, G. J. FARROW, D. JACKSON, G. WOSTENHOLM and B. YATES, *J. Thermoplastic Compos. Mater.* **3** (1990) 66–80.
3. J. A. BARNES, I. J. SIMMS, G. J. FARROW, D. JACKSON, G. WOSTENHOLM and B. YATES, *J. Mater. Sci.* **26** (1990) 2259–2271.
4. J. M. GAITONDE and M. V. LOWSON, *Compos. Sci. Technol.* **40** (1991) 69–85.
5. G. SCHWARZ, F. KRAHN and G. HARTWIG, *Cryogenics* **31** (1991) 244–247.
6. R. S. RAGHAVA, *Polym. Compos.* **9** (1988) 1–11.
7. P. S. TURNER, *Res. National Bureau of Standards*, **37** (1946) 239.
8. R. A. SCHAPERY, *J. Compos. Mater.* **2** (1968) 380–404.
9. N. J. CHAMBERLAIN, British Aircraft Corporation Report SON(P) (1968) 33.
10. B. W. ROSEN, PhD dissertation, University of Pennsylvania, (1968).
11. B. W. ROSEN and Z. HASHIN, *Int. J. Engng. Sci.* **8** (5) (1970) 157–173.
12. J. ABOUDI, *Appl. Mech. Rev.* **42** (7) (1989) 193–221.
13. R. M. CHRISTIENSEN, "Mechanics of composite materials", (Wiley, New York, 1979).
14. O. PIRGON, G. WOSTENHOLM and B. YATES, *J. Phys. D.* **6** (1973) 309.
15. ICI fiberite data sheet.
16. G. J. FARROW, G. H. WOSTENHOLM, M. I. DARBY and B. YATES, *J. Mater. Sci. Lett.* **9** (1990) 743–744.
17. T. J. CHAPMAN, J. W. GILLESPIE, J. A. E. MANSON, R. B. PIPES and J. C. SEFERIS, Proceedings of the American Society for Composites, Third Technical Conference, Blacksburg, Va, (Technomic Publishing, 1988, 449–458).
18. T. J. CHAPMAN, J. W. GILLESPIE JR, R. B. PIPES, J. A. E. MANSON and J. C. SEFERIS, *J. Comp. Mater.* **24** (1990) 616–643.
19. J. A. BARNES, G. BYERLY, M. C. LEBOUTON and N. ZAHLAN, *Compos. Manuf.* **2** (3/4) (1991) 171–179.
20. J. A. BARNES and G. E. BYERLY, The Formation of Residual Stresses in Laminated Thermoplastic Composites, Submitted to *Comp. Sci. Technol.* August (1992).
21. P. M. SHEAFFER, Proceedings of the Eighteenth Biennial Conference on Carbon, (1987) pp. 20–21.

Received 1 February 1993
and accepted 24 February 1993